Generalized fast marching method for computing highest threatening trajectories with curvature constraints and detection ambiguities in distance and radial speed

Frédéric Barbaresco, François Desquilbet, Johann Dreo, Jean-Marie Mirebeau

Generalized fast marching method for computing highest threatening trajectories with curvature constraints and detection ambiguities in distance and radial speed

Frederic Barbaresco*, François Desquibet†, Johann Dreo‡, Jean-Marie Mirebeau§

October 17, 2019

Abstract

We present a recent numerical method devoted to computing curves that *globally minimize* an energy featuring both a *data driven* term, and a second order *curvature penalizing* term. Applications to image segmentation are discussed. We then describe in detail recent progress on radar network configuration, in which the optimal curves represent an opponent's trajectories.

1 Globally optimal paths with a curvature penalty

This paper is concerned with planar paths minimizing certain energy functionals, between two given points and with prescribed tangents at these points. The path energy model features a low order data-driven term, and a higher order regularization term. A globally optimal path is found, using optimal control techniques, which involve numerically solving a PDE on the configuration space of positions and orientations. We discuss applications to image segmentation, and motion planning in §2Threatening trajectories and radar network configurationsection.2.

Path energy models In the models of interest to us, the cost of a smooth planar path $\mathbf{x} : [0, T] \to \Omega$, parametrized by Euclidean arc length and within a domain $\Omega \subset \mathbb{R}^2$, takes the following form:

$$\mathfrak{C}(\mathbf{x}) := \int_0^T \alpha(\mathbf{x}(s), \dot{\mathbf{x}}(s))\, \mathcal{C}(\|\ddot{\mathbf{x}}(s)\|)\, \mathrm{d}s. \tag{1}$$

We denoted by $\alpha : \overline{\Omega} \times \mathbb{S}^1 \to]0, \infty[$ an arbitrary continuous data-driven term, depending on the path position and direction. The path local curvature $\kappa = \|\ddot{\mathbf{x}}(t)\|$ (recall that $\|\dot{\mathbf{x}}(s)\| \equiv 1$) is penalized in (1.1Path energy modelsequation.1.1) by a cost function $\mathcal{C}(\kappa)$, which may be chosen among the following classical models, here sorted by increasingly stiffness:

$$\text{Reeds-Shepp: } \sqrt{1+\kappa^2}, \qquad \text{Euler-Mumford: } 1+\kappa^2, \qquad \text{Dubins: } \begin{cases} 1 & \kappa \leq 1, \\ \infty & \text{else.} \end{cases} \tag{2}$$

*Thales Land & Air Systems
†Ecole Normale Supérieure de Paris
‡Thales Research and Technology, Palaiseau
§University Paris-Sud, CNRS, University Paris-Saclay, F-91405, Orsay
This project was partly support by ANR research grant MAGA, ANR-16-CE40-0014

They are respectively representative of (i) a wheelchair-like robot, (ii) the bending energy of an elastic bar, and (iii) a vehicle with a bounded turning radius. In the case of the Reeds-Shepp model, one must further distinguish between the classical model with reverse gear, and the forward only variant [6].

Viscosity solutions, and the Fast marching algorithm. Data-driven path energies, subject to e.g. fixed endpoints, usually possess many local minima. In order to guarantee that the global minimum is found, path energy minimization must be reformulated as an optimal control problem. The corresponding value function is the unique viscosity solution to a PDE of eikonal type, and the optimal paths can be extracted by backtracking once it is numerically computed [13].

Only simple first order energies, such as $\int_0^T \alpha(\mathbf{x}(s))\|\dot{\mathbf{x}}(s)\|\mathrm{d}s$ could originally be addressed in the viscosity solution framework, typically using the Fast Marching Method (FMM) which solves the eikonal PDE in a single pass over the domain [4]. Recent progress [6, 3, 10] enabled the extension to (1.1Path energy modelsequation.1.1) of the FMM. For that purpose the path is lifted in the configuration space of positions and orientations, defining $\gamma(t) = (\mathbf{x}(t), \theta(t))$ subject to the constraint $\dot{\mathbf{x}}(t) = \mathbf{n}(\theta(t))$ where $\mathbf{n}(\theta) := (\cos\theta, \sin\theta)$. This non-holonomic constraint allows to reformulate (1.1Path energy modelsequation.1.1) as a first order energy, since $|\ddot{\mathbf{x}}(t)| = |\dot{\theta}(t)|$. The energy of a non-admissible path $\gamma = (\mathbf{x}, \theta) : [0,1] \to \mathbb{R}^2 \times \mathbb{S}^1$, defined in the augmented space but such that $\dot{\mathbf{x}}(t)$ is not positively proportionnal to $\mathbf{n}(\theta(t))$ for some $t \in [0,1]$, is defined as $+\infty$. See [10] for details and comparison with alternative approaches such as [15, 9].

At the request of a reviewer, we do provide some additional detail on the theoretical and numerical approach. Denote by $u(\mathbf{x}, \theta)$ the minimal cost (1.1Path energy modelsequation.1.1) of a path from the domain boundary $\partial\Omega$ to the endpoint $\mathbf{x}$ with final tangent $(\cos\theta, \sin\theta)$. Then u, known as the value function to the optimal control problem, is a (possibly discontinuous) viscosity solution [2, 10] to the Bellman equation

$$\mathcal{F}^*_{(\mathbf{x},\theta)}(\nabla u(\mathbf{x},\theta)) = \alpha(\mathbf{x},\theta) \quad \text{in } \Omega \times \mathbb{S}^1, \qquad\qquad u(\mathbf{x},\theta) = 0 \quad \text{on } \partial\Omega \times \mathbb{S}^1,$$

where the α is the data-driven term appearing in (1.1Path energy modelsequation.1.1). The Hamiltonian $\mathcal{F}^*$ in the l.h.s. has the following expression: denoting $\hat{x} := \langle \nabla_{\mathbf{x}} u(\mathbf{p}), \mathbf{n}(\theta)\rangle$ and $\hat{\theta} := \partial_\theta u(\mathbf{p})$

$$\text{Reeds-Shepp: } \sqrt{\hat{x}_+^2 + \hat{\theta}^2}, \qquad \text{Euler-Mumford: } \hat{x} + \sqrt{\hat{x}^2 + \hat{\theta}^2}, \qquad \text{Dubins: } \max\{0,\, \hat{x} + \hat{\theta},\, \hat{x} - \hat{\theta}\}.$$

These expressions are derived from the curvature dependent cost $\mathcal{C}$ (1.2Path energy modelsequation.1.2) as $\sup\{(\hat{x} + \hat{\theta}\kappa)/\mathcal{C}(\kappa);\, \kappa \in \mathbb{R}\}$. Using adequate techniques, we approximate this Hamiltonian in the following generic form

$$\mathcal{F}^*_{(\mathbf{x},\theta)}(\nabla u(\mathbf{x},\theta))^2 \approx \max_{1\le k\le K} \left(\sum_{1\le i\le I} \alpha_{ik}(\theta) \langle \nabla u(\mathbf{x},\theta), \mathbf{e}_{ik}(\theta)\rangle^2 + \sum_{1\le j\le J} \beta_{jk}(\theta) \max\{0, \langle \nabla u(\mathbf{x},\theta), \mathbf{f}_{jk}(\theta)\rangle\}^2 \right), \tag{3}$$

where the weights α_{ik}, β_{jk}, are *non-negative*, and the offsets $\mathbf{e}_{ik}, \mathbf{f}_{jk}$ have *integer* coordinates. The directional derivatives are then approximated using upwind finite differences as in (1.4Viscosity solutions, and the Fast m below, and the coupled system of equations resulting from the discretized PDE is solved in a single pass over the domain [12]. It would be too long to describe here the approximation procedure [10, 12] yielding (1.3Viscosity solutions, and the Fast marching algorithmequation.1.3), which involves a relaxation parameter $\varepsilon > 0$ and techniques from algorithmic geometry. Nevertheless let us mention the meta parameters (I, J, K) used: Reeds-Shepp $(1, 3, 1)$, Euler-Mumford $(0, 27, 1)$, Dubins $(0, 6, 2)$.

For comparison, the standard d-dimensional isotropic fast marching method [13] can be framed in a similar setting, with $(I, J, K) = (d, 0, 1)$: denoting by $(\mathbf{e}_i)_{i=1}^d$ the canonical basis of $\mathbb{R}^d$

$$\|\nabla u(\mathbf{x})\|^2 = \sum_{1\leq i\leq d} \langle \nabla u(x), \mathbf{e}_i\rangle^2 \approx \sum_{1\leq i\leq d} \max\Big\{0, \frac{u(\mathbf{x}) - u(\mathbf{x} - h\mathbf{e}_i)}{h}, \frac{u(\mathbf{x}) - u(\mathbf{x} + h\mathbf{e}_i)}{h}\Big\}^2. \quad (4)$$

Applications to image processing. Image segmentation methods based on active contours typically involve path energies balancing low-order data-driven terms, and higher order regularization terms. Unfortunately, many second order models can only be locally optimized [8], resulting in spurious local minima and high sensitivity to initialization. In contrast, first order models [4] can be globally optimized using the FMM, but the lack of smoothness penalization gives way to various artefacts referred to as leaks, shortcuts, and branches combination problems [3].

Our numerical method combines the best of the two worlds: a second order energy model (1.1Path energy models and fast global minimization, with prescribed endpoint positions and tangents. This enables new developments, see for instance [3] on the retina vessel tree segmentation, and [6] on white matter fiber path extraction.

2 Threatening trajectories and radar network configuration

In a collaboration work with the company Thales, we optimize the configuration of a radar network for protecting an objective within a region, against an enemy assumed to have unlimited intelligence and computing power, and yet whose vehicle is subject to some manoeuverability constraints. The goal is to maximize the probability of detection of the most dangerous trajectory between a given source and target, which will take advantage of any hideout in the terrain, blind spot or physical limitation in the radar network. The trajectory is only subject to a lower bound in the turning radius, due to the vehicle high speed. See also the companion paper [5].

We model this problem as a non-cooperative zero-sum game: a first player chooses a setting ξ for the radar detection network Ξ, and the other player chooses a trajectory γ from the admissible class Γ with full information over the network ξ. The players' objective is respectively to maximize and minimize the path cost:

$$C(\Xi, \Gamma) := \sup_{\xi\in\Xi} \inf_{\gamma\in\Gamma} \mathfrak{C}_\xi(\gamma)$$

where $\mathfrak{C}_\xi$ is the function $\mathfrak{C}$ defined in (1.1Path energy modelsequation.1.1) but with a data-driven cost term α_ξ depending on the setting ξ of the network, and accounting for the local probability of detection. Minimization over $\gamma \in \Gamma$ (given $\xi \in \Xi$) is performed using the fast and reliable techniques of §1Globally optimal paths with a curvature penaltysection.1. We rely on the CMA-ES algorithm [7] for the subsequent optimization over $\xi \in \Xi$, which is rather difficult (non-convex, non-differentiable).

In comparison with earlier works [1, 16], we use the curvature bounded Dubins model (1.2Path energy modelsequation.1.2, right) to reject non-physical attacking trajectories, featuring e.g. angular turns or oscillations in the vehicle direction. We also considerably improve, relative to [11], the detection probability model, used to define $\alpha_\xi(\mathbf{x}, \dot{\mathbf{x}})$, taking into account the three following factors respectively related to the radar, the target, and the terrain [14].

- The *blindness map* accounts for the probability of detection of a generic target by a radar, depending on the distance and the radial speed of the target relatively to the radar, see Figure 1., left. There are blind areas, due to the fact that a radar cannot listen to its signal while emitting it, and to the Doppler effect, which respectively causes blind radial distances and blind

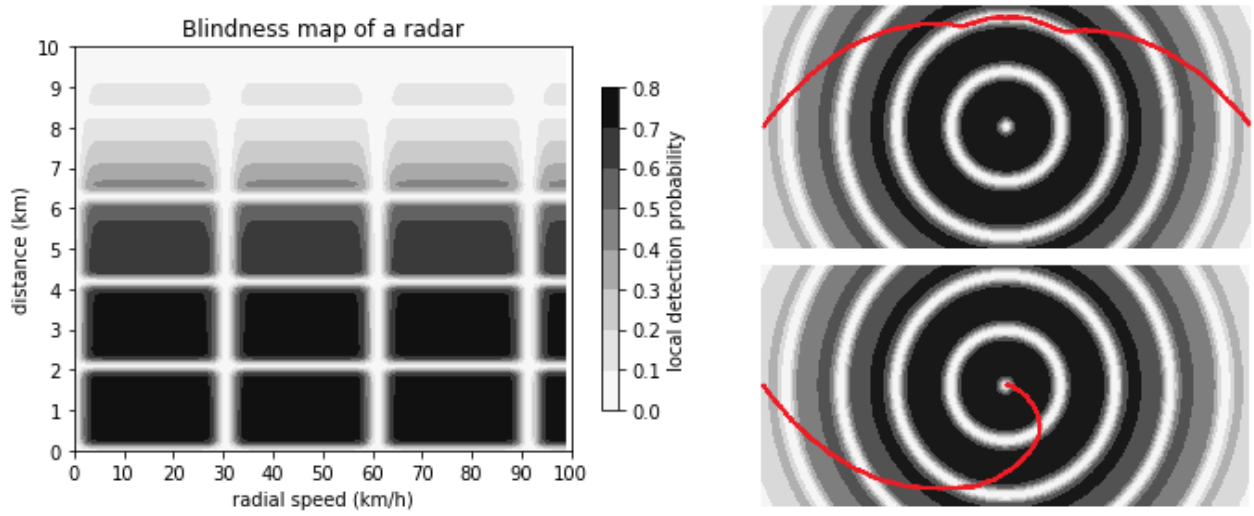

Figure 1: (left) blindness map of a radar (simulated data). (top right) dodging a radar through a blind distance, (bottom right) spiraling threatening trajectory

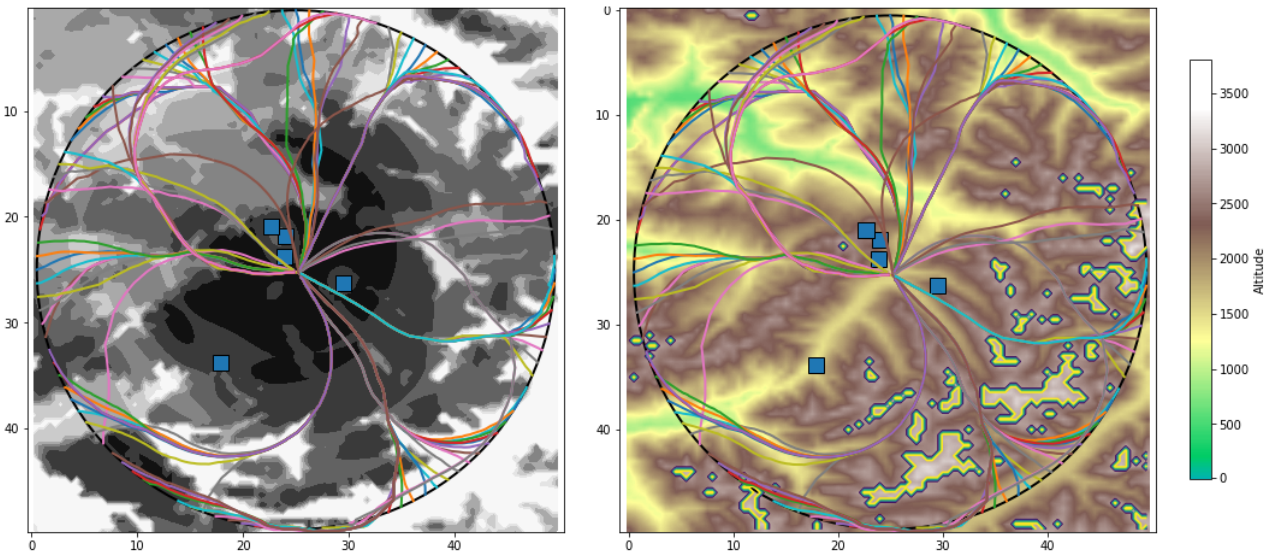

Figure 2: Threatening trajectories, from a circular region towards its center point, with optimized radar positions. (left) Positional factor $\alpha_\xi(\mathbf{x})$ in the cost map, where ξ is the radar configuration. (right) Digital elevation map.

radial speeds. The positions of the blind areas are periodical and depend on internal parameters of the radar that can be optimized: signal wavelength, and pulse repetition interval.

- The *radar cross section* accounts for the probability of detection of a specific target, depending on its orientation relative to the radar. For instance, a furtive plane often has a low probability of detection if seen from the front, and a higher one if seen from the side.

- The *elevation map* is used to determine blind regions in the terrain due to obstruction of the radar line of sight. In a mountainous area, a target can take advantage of valleys to move "under the radar". The Earth curvature is also taken into account.

The profile of the cost function with regard to the direction of movement is typically non-convex, which is significant only in the presence of a curvature penalization. For that, we choose the Dubins model, in which the curvature radius is bounded. We showcase the following three phenomena.

- Trajectories dodging radars through their blind distances (cf Figure 1., top right). In this picture, only the positional factor in the cost map is shown in greyscale, and not the part of the cost depending on the orientation. The red line represents the optimal trajectory of the target, going from the left to the right of a rectangular domain, with a radar in the center. It features a circle arc, at a precise blind distance from the radar, and two spiral arcs, see below.

- Spiraling threatening trajectories, taking advantage of the blind radial speed (cf Figure 1., bottom right). The red line represents the trajectory of the target, going from the left to the center of the domain where the radar is located, maintening a constant angle with the radar in order to minimize visibility, except at the end due to the imposed bound on path curvature.

- Hiding in valleys (cf Figure 2.). A digital elevation map, of 50km×50km around the city of Davos in the Alps, is used to construct a probability of detection map, see Figure 2Threatening trajectories, from a circular region towards its center point, with optimized radar positions. (left) Positional factor $\alpha_\xi(\mathbf{x})$ in the cost map, where ξ is the radar configuration. (right) Digital elevation map.figure.caption.5. Threatening trajectories tend to concentrate in valleys. The optimized radar positions are close to the target to be defended, and either on high ground or in alignment with long valleys.

Future works will be devoted to further enhancing the model, taking into account limited knowledge of the attacker (e.g. due to the use of passive radar receivers), introducing success criteria more complex than mere detection (e.g. requiring detection early enough for interception), and considering speed and altitude variations along the trajectory.

References

[1] F Barbaresco. Computation of most threatening radar trajectories areas and corridors based on fast-marching & Level Sets. In *IEEE Symposium On Computational Intelligence For Security And Defence Applications*, pages 51–58. IEEE, 2011.

[2] Martino Bardi and Italo Capuzzo-Dolcetta. *Optimal control and viscosity solutions of Hamilton-Jacobi-Bellman equations*. Springer Science & Business Media, 2008.

[3] Da Chen, Jean-Marie Mirebeau, and Laurent D. Cohen. Global Minimum for a Finsler Elastica Minimal Path Approach. *International Journal of Computer Vision*, 122(3):458–483, 2017.

[4] Laurent D Cohen and R Kimmel. Global minimum for active contour models: A minimal path approach. *International Journal of Computer Vision*, 24(1):57–78, 1997.

[5] Johann Dreo, François Desquilbet, Frederic Barbaresco, and Jean-Marie Mirebeau. Netted multi-function radars positioning and modes selection by non-holonomic fast marching computation of highest threatening trajectories. In *International RADAR'19 conference*. IEEE, September 2019.

[6] Remco Duits, Stephan PL Meesters, Jean-Marie Mirebeau, and Jorg M Portegies. Optimal paths for variants of the 2D and 3D Reeds-Shepp car with applications in image analysis. *Journal of Mathematical Imaging and Vision*, pages 1–33, 2018.

[7] Nikolaus Hansen, Sibylle D Müller, and Petros Koumoutsakos. Reducing the time complexity of the derandomized evolution strategy with covariance matrix adaptation (CMA-ES). *Evolutionary computation*, 11(1):1–18, 2003.

[8] Michael Kass, Andrew Witkin, and Demetri Terzopoulos. Snakes: Active contour models. *International Journal of Computer Vision*, 1(4):321–331, January 1988.

[9] Wei Liao, Karl Rohr, and Stefan W o rz. Globally Optimal Curvature-Regularized Fast Marching For Vessel Segmentation. *Medical Image Computing and Computer-Assisted Interventation-MICCAI 2013. Springer Berlin Heidelberg.*, pages 550–557, 2013.

[10] Jean-Marie Mirebeau. Fast-marching methods for curvature penalized shortest paths. *Journal of Mathematical Imaging and Vision*, pages 1–32, 2017.

[11] Jean-Marie Mirebeau and Johann Dreo. Automatic differentiation of non-holonomic fast marching for computing most threatening trajectories under sensors surveillance. In Frank Nielsen and Frédéric Barbaresco, editors, *Geometrical Science of Information*, April 2017.

[12] Jean-Marie Mirebeau and Jorg Portegies. Hamiltonian fast marching: A numerical solver for anisotropic and non-holonomic eikonal pdes. *Image Processing On Line*, 9:47–93, 2019.

[13] James A. Sethian. A fast marching level set method for monotonically advancing fronts. *Proceedings of the National Academy of Sciences*, 93(4):1591–1595, 1996.

[14] Merrill Ivan Skolnik. *Radar handbook*. 1970.

[15] Petter Strandmark, Johannes Ulen, Fredrik Kahl, and Leo Grady. Shortest Paths with Curvature and Torsion. In *2013 IEEE International Conference on Computer Vision (ICCV)*, pages 2024–2031. IEEE, 2013.

[16] Christopher Strode. Optimising multistatic sensor locations using path planning and game theory. In *IEEE Symposium On Computational Intelligence For Security And Defence Applications*, pages 9–16. IEEE, 2011.